Electronic Supplementary Information:

Non-invasive and label-free identification of human natural killer subclasses by biophysical single-cell features in microfluidic flow

David Dannhauser,[a] Domenico Rossi,[b] Anna Teresa Palatucci,[c] Valentina Rubino,[d] Flavia Carriero,[d] Giuseppina Ruggiero,[d] Mimmo Ripaldi,[e] Mario Toriello,[e] Giovanna Maisto,[e] Paolo Antonio Netti,[ab] Giuseppe Terrazzano[c] and Filippo Causa*[a]

[a]*Interdisciplinary Research Centre on Biomaterials (CRIB) and Dipartimento di Ingegneria Chimica, dei Materiali e della Produzione Industriale, Università degli Studi di Napoli "Federico II", Piazzale Tecchio 80, 80125 Naples, Italy.*
[b]*Center for Advanced Biomaterials for Healthcare@CRIB, Istituto Italiano di Tecnologia, Largo Barsanti e Matteucci 53, 80125 Naples, Italy.*
[c]*Dipartimento di Scienze (DiS), Università della Basilicata, Via dell'Ateneo Lucano 10, 85100 Potenza, Italy.*
[d]*Dipartimento di Scienze Mediche Traslazionali, Università degli Studi di Napoli "Federico II", Naples, Italy.*
[e]*Dipartimento Oncologia AORN Santobono Pausilipon Hospital, Via Posillipo, 226, 80123, Naples, Italy.*
**Correspondence and request for material should be addressed to F.C. (email: filippo.causa@unina.it)*

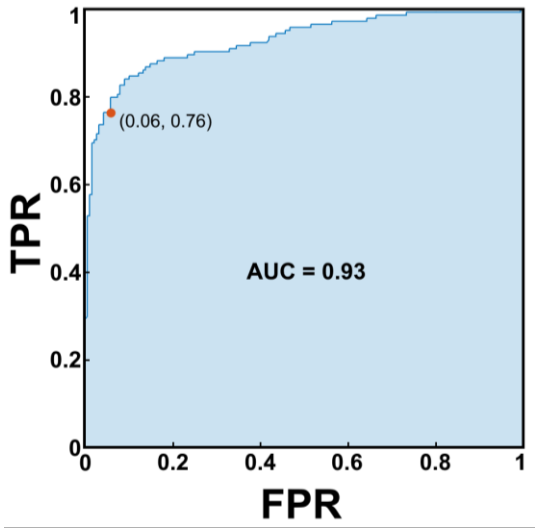

Fig. S1. Receiver Operating Characteristic (ROC). True Positive Rate (TPR) versus False Positive Rate (FPR) is shown for CD56^{bright} and CD56^{dim} NK cells. The plot shows positive class CD56^{dim} versus negative class CD56^{bright}.

Table S1. Detailed results of NK classifier training. Values of Sensitivity, Specificity, Positive Predictive value (PP), Negative Predicted value (NP), and Accuracy for ML results applied on healthy probands. True Positive rate (TP), False Positive rate (FP), True Negative rate (TN) and False Negative rate (FN) are also indicated for both CD56^{bright} and CD56^{dim} cells.

	Sensitivity	Specificity	PP	NP	Accuracy	TP	FP	TN	FN
CD56^{bright}	96.81%	79.17%	85.85%	95.00%	89.16%	182	30	114	6
CD56^{dim}	79.17%	96.81%	95.00%	85.85%	89.16%	114	6	182	30

Table S2. Values of biophysical properties of cells from the four healthy donors. Detailed average values of all the four biophysical properties from the four probands (A-B-C-D) are shown, together with standard deviation.

Sample	D	STDev	N/C-ratio	STDev	RI_N	STDev	RI_C	STDev
A – NK	6.74	1.16	0.957	0.014	1.405	0.007	1.361	0.003
A – $CD56^{dim}$	6.59	1.09	0.958	0.014	1.403	0.005	1.360	0.002
A – $CD56^{bright}$	7.43	1.22	0.956	0.015	1.414	0.006	1.365	0.005
B – NK	9.06	0.72	0.953	0.010	1.403	0.006	1.360	0.001
B – $CD56^{dim}$	8.93	0.68	0.952	0.008	1.400	0.000	1.360	0.001
B – $CD56^{bright}$	9.47	0.70	0.953	0.016	1.412	0.004	1.360	0.000
C – NK	8.89	0.84	0.955	0.015	1.404	0.006	1.362	0.004
C – $CD56^{dim}$	8.87	0.91	0.955	0.015	1.401	0.003	1.361	0.004
C – $CD56^{bright}$	8.95	0.68	0.954	0.014	1.412	0.004	1.363	0.005
D – NK	8.04	1.15	0.944	0.021	1.403	0.005	1.361	0.002
D – $CD56^{dim}$	7.87	1.14	0.942	0.020	1.400	0.002	1.360	0.001
D – $CD56^{bright}$	8.52	1.07	0.950	0.024	1.410	0.002	1.362	0.004

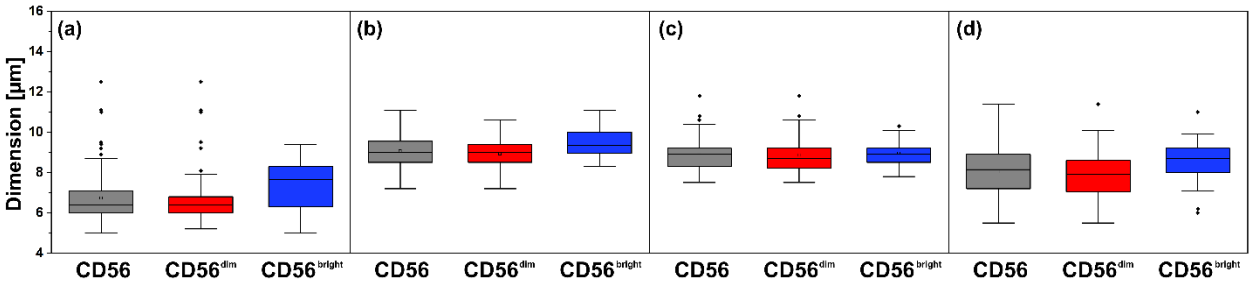

Fig. S2: The cell dimension for all four probands is shown. The NK value indicates the cell dimension before the ML classification, while $CD56^{brigth}$ and $CD56^{dim}$ values retrieve from the ML outcome.

Table S3. Values of biophysical features of cells from the G-CSF mobilized cells. Detailed average values of all the four biophysical features from the mobilized cells sample are shown at seven different timesteps of IL-15 stimulation.

Sample	D	STDev	N/C-ratio	STDev	RI_N	STDev	RI_C	STDev
0h – NK	7.74	± 0.81	0.97	± 0.01	1.416	± 0.012	1.360	± 0.000
0h – $CD56^{dim}$	7.24	± 0.70	0.95	± 0.01	1.401	± 0.005	1.360	± 0.000
0h – $CD56^{bright}$	7.98	± 0.75	0.97	± 0.01	1.423	± 0.005	1.360	± 0.000
12h IL15 – NK	8.05	± 1.14	0.93	± 0.06	1.407	± 0.005	1.363	± 0.005
12h IL15 – $CD56^{dim}$	8.10	± 1.34	0.92	± 0.07	1.405	± 0.006	1.363	± 0.006
12h IL15 – $CD56^{bright}$	7.98	± 0.74	0.94	± 0.03	1.410	± 0.000	1.362	± 0.004
24h IL15 – NK	7.62	± 1.33	0.94	± 0.04	1.408	± 0.006	1.361	± 0.004
24h IL15 – $CD56^{dim}$	7.77	± 1.59	0.94	± 0.05	1.405	± 0.006	1.362	± 0.005
24h IL15 – $CD56^{bright}$	7.44	± 0.92	0.94	± 0.02	1.411	± 0.003	1.360	± 0.002
48h IL15 – NK	7.93	± 1.99	0.89	± 0.07	1.413	± 0.007	1.370	± 0.007

48h IL15 – CD56^{dim}	8.73	± 2.46	0.85	± 0.08	1.412	± 0.008	1.372	± 0.008
48h IL15 – CD56^{bright}	7.23	± 1.06	0.94	± 0.03	1.413	± 0.006	1.369	± 0.006
72h IL15 – NK	8.77	± 2.07	0.89	± 0.06	1.412	± 0.007	1.376	± 0.007
72h IL15 – CD56^{dim}	9.30	± 2.10	0.87	± 0.06	1.412	± 0.007	1.378	± 0.007
72h IL15 – CD56^{bright}	7.55	± 1.43	0.93	± 0.04	1.412	± 0.006	1.373	± 0.006
96h IL15 – NK	8.65	± 1.51	0.85	± 0.07	1.409	± 0.008	1.379	± 0.006
96h IL15 – CD56^{dim}	8.85	± 1.50	0.83	± 0.06	1.409	± 0.008	1.379	± 0.006
96h IL15 – CD56^{bright}	7.59	± 1.13	0.92	± 0.03	1.411	± 0.008	1.377	± 0.005
120h IL15 – NK	8.31	± 1.28	0.81	± 0.06	1.411	± 0.005	1.378	± 0.005
120h IL15 – CD56^{dim}	8.41	± 1.31	0.81	± 0.05	1.411	± 0.005	1.379	± 0.004
120h IL15 – CD56^{bright}	7.51	± 0.70	0.89	± 0.03	1.411	± 0.005	1.374	± 0.005
120h – NK	7.10	± 0.94	0.96	± 0.02	1.410	± 0.007	1.360	± 0.002
120h – CD56^{dim}	6.87	± 0.58	0.96	± 0.02	1.405	± 0.005	1.360	± 0.002
120h – CD56^{bright}	7.23	± 1.09	0.95	± 0.02	1.413	± 0.007	1.360	± 0.002

Table S4. Brightfield measurement of cell dimensions. Investigations regarding IL-15 treatment of NKs. Measurement of NK treated with IL-15 was performed from 0 to 120h using a bright field microscope.

	Time 0	**Time 12h**	**Time 24h**	**Time 48h**	**Time 72h**	**Time 96h**	**Time 120h**
Diameter (μm)	8.84 ± 0.91	7.87 ± 1.12	8.25 ± 0.79	8.68 ± 0.98	9.07 ± 1.14	9.76 ± 1.33	9.24 ± 1.42
Nucleus (μm)	5.23 ± 0.66	4.71 ± 0.91	5.08 ± 0.68	5.22 ± 0.85	5.63 ± 1.16	5.86 ± 1.21	5.06 ± 1.26
n/c ratio	0.60 ± 0.08	0.60 ± 0.11	0.62 ± 0.09	0.60 ± 0.11	0.62 ± 0.09	0.60 ± 0.10	0.55 ± 0.10

Table S5. 'Trypan blue' test for CD56^{brigth} and CD56^{dim} NKs. We evaluated the death ratio of CD56^{brigth} and CD56^{dim} after cytometer separation with a Trypan blue test (see Fig S4).

	Not stained (alive)	**Stained (damaged)**	**% stained (damaged)**
CD56^{brigth}	67	2	3
CD56^{dim}	9	2	18
total	76	4	5

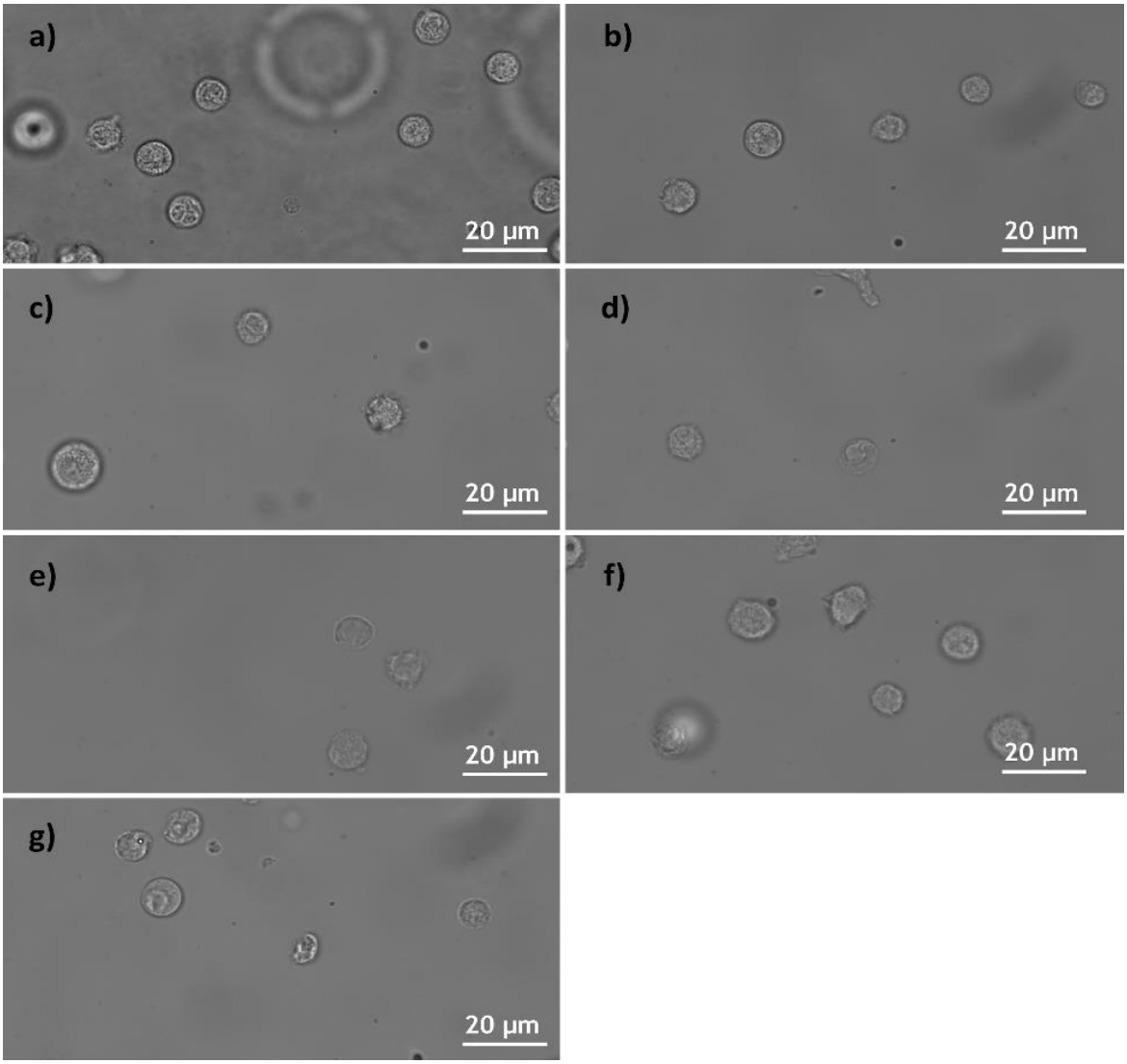

Fig. S3. Brightfield images of mobilized cells at different timesteps of IL-15 treatment. Images of NK treated with IL15 from time 0 (a) to time 120h (g) using a bright-field microscope (100 × objective, X81, Olympus).

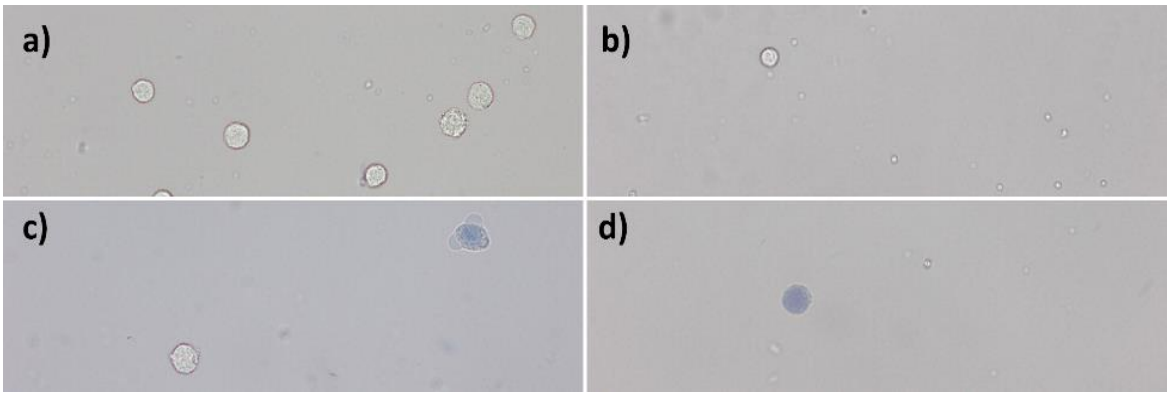

Fig. S4. **'**Trypan blue' test for CD56^{brigth} and CD56^{dim} NKs. a) unstained CD56^{dim} NK, b) unstained CD56^{brigth} NK, c) stained CD56^{dim} NK, d) stained CD56^{dim} NK cells using a bright-field microscope (20 × objective, BX53, Olympus).

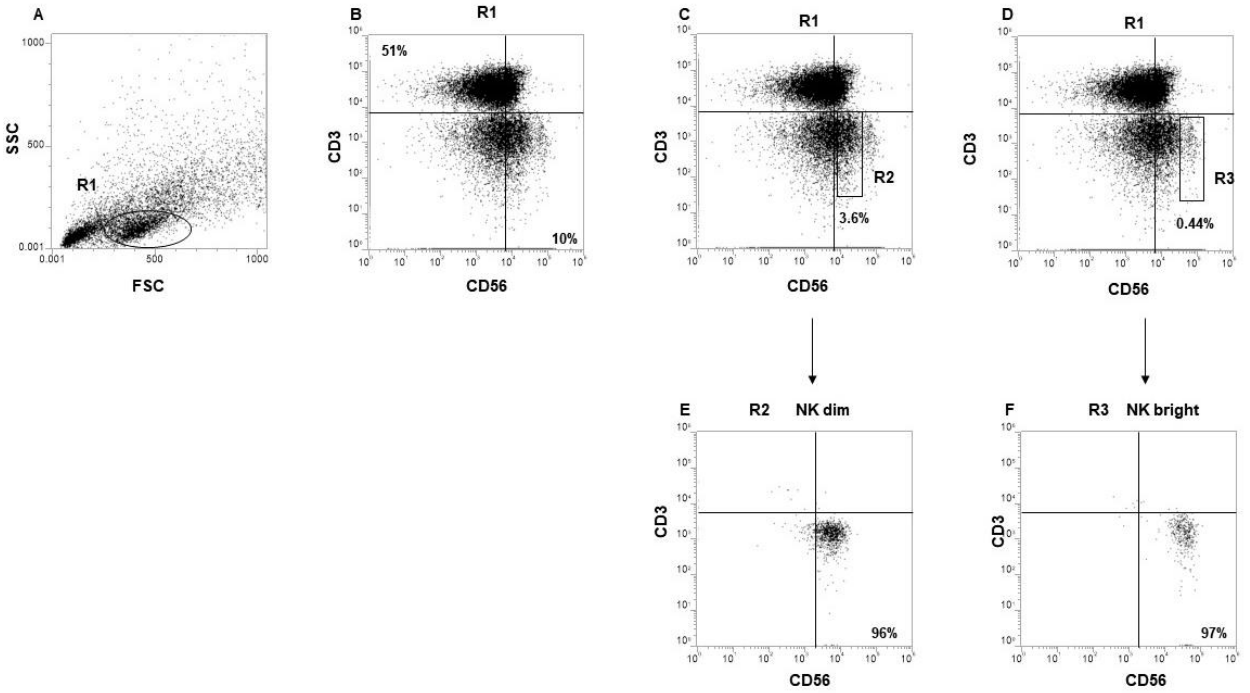

Fig. S5. Cytometer measurement to assess purity of NK and NK subclasses isolation from sample of blood bank of the medical school of the Federico II university of Naples (Italy). NK subclasses were purified starting from PBMC gated on the lymphocyte region (R1 in Panel A) and evaluated for the percentage of T-lymphocytes ($CD3^+$ $CD56^-$ cells in upper left quadrant of Panel B, approximately 51% of the whole lymphocyte population) and NK cells ($CD3^-$ $CD56^+$ in lower right quadrant of Panel B, approximately 10% of the whole lymphocyte population). Subsequently, NK cells were separated by a flow cytometry gating strategy for the exclusive positivity to the CD56 marker, in terms of *dim* (R2 in Panel c) and *bright* (R3 in Panel D) fluorescence intensity, in order to obtain the sorted $CD56^{dim}$ (Panel E) and $CD56^{bright}$ (Panel F) NK subclasses. Panel A shows the cell size value (FSC = forward scatter) on the x axis and the cell complexity value (SSC = side scatter) on the y axis. Panels B-F report the fluorescence intensity for the CD56 (*x* axis) and CD3 (*y* axis). The data represent the results obtained in one out of four independent experiments. The vertical arrows indicate the transition from the mixed population $CD56^{dim}$ and $CD56^{bright}$, before sorting, to single $CD56^{dim}$ (transition from C to E Panels) and $CD56^{brigh}$ (transition from D to F Panels) NK subclasses after sorting.

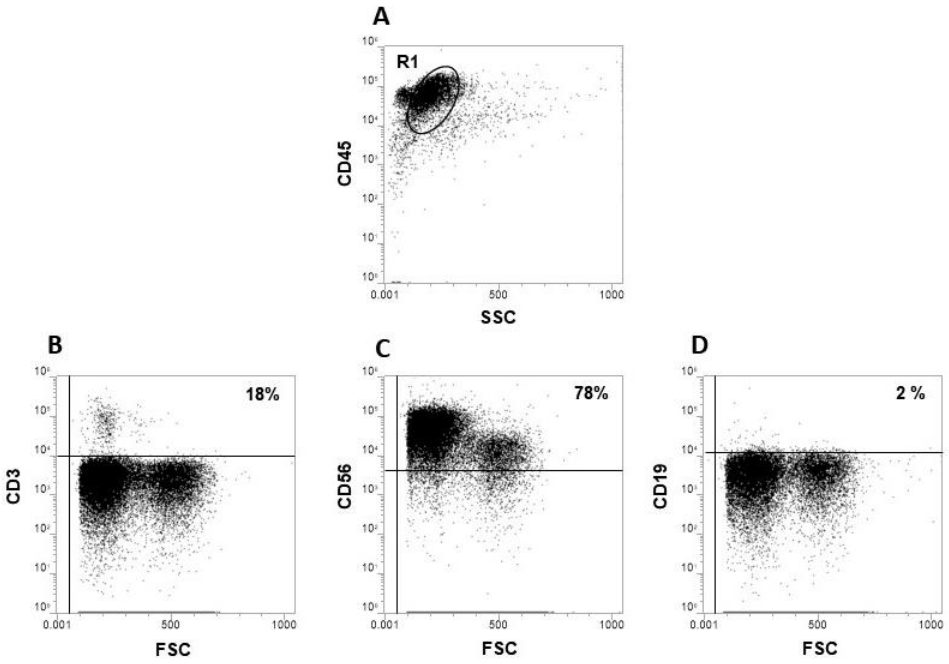

Fig. S6. Flow Cytometer analysis of mobilized NK from sample of Santobono-Pausilipon Hospital, Department of Pediatric Hemato-Oncology. Analysed ells were gated on the $CD45^+$ lymphocyte region (R1 in Panel A) and evaluated for the percentage of T-lymphocytes ($CD3^+$ cells in upper right quadrant of Panel B, approximately 18 % of the R1 population), NK cells ($CD56^+$ in upper right quadrant of Panel C, approximately 78 % of R1 population) and B-lymphocytes ($CD19^+$ in upper right quadrant of Panel D, approximately 2% of R1 population). The *x* axis reports the cell complexity value (SSC = side scatter) in Panel A and the cell size value (FSC = forward scatter) in Panels B-D. The *y* axis reports the fluorescence intensity for the CD45 (Panel A), CD3 (Panel B), CD56 (Panel C) and CD19 (Panel D). The data represent the results obtained in one independent experiment. Note that the flow cytometric revealed a double population of NK lymphocytes ($CD56^+$ in upper right quadrant of Panel C): a larger one (about 30% of the CD56 positive cells) and a smaller one (about 70%) of CD56 positive cells).